Proceedings of Equadiff-11
2005, pp. 87–95
ISBN 978-80-227-2624-5

HIGHER ORDER METHOD FOR THE NUMERICAL SOLUTION OF THE COMPRESSIBLE EULER EQUATIONS*

MILOSLAV FEISTAUER† AND VÁCLAV KUČERA‡

Abstract. This paper is concerned with a numerical technique for the solution of inviscid compressible flow with a wide range of Mach numbers. It is based on the use of the discontinuous Galerkin finite element method applied to the Euler equations written in the conservative form, a semi-implicit time discretization and characteristics-based boundary conditions, which are transparent for acoustic phenomena. For transonic flows, additional shock capturing terms are added in order to avoid the Gibbs phenomenon near shock waves.

Key words. compressible inviscid flow, Euler equations, discontinuous Galerkin finite element method,semi-implicit time discretization, low Mach number flow, transonic flow

AMS subject classifications. 65M60, 76B99, 76H05

1. Introduction. In the numerical solution of compressible flow, it is necessary to overcome a number of obstacles. Let us mention the necessity to resolve accurately shock waves, contact discontinuities and (in viscous flow) boundary layers, wakes and their interaction. Some of these phenomena are connected with the simulation of high speed flow with high Mach numbers. However, it appears that the solution of low Mach number flow is also rather difficult. This is caused by the stiff behaviour of numerical schemes and acoustic phenomena appearing in low Mach number flows at incompressible limit. In this case, standard finite volume schemes fail. This led to the development of special finite volume techniques allowing the simulation of compressible flow at incompressible limit, which is based on modifications of the Euler or Navier-Stokes equations. (See, e. g. [13], [15], [18, Chapter 14], or [14, Chapter 5].)

Here we are concerned with the development of an efficient, robust and accurate method allowing the solution of compressible flow with a wide range of the Mach number without any modification of the governing equations. This technique is based on the *discontinuous Galerkin finite element method* (DGFEM), which can be considered as a generalization of the finite volume as well as finite element methods, using advantages of both these techniques. It employs piecewise polynomial approximations without any requirement on the continuity on interfaces between neighbouring elements. (For various applications of the DGFEM to compressible flow, see e. g. [1], [2], [3], [4], [11], [16]. Theory of the DGFEM applied to nonlinear nonstationary convection diffusion problems can be found in [5], [6] and [8].) The discontinuous Galerkin space semidiscretization is combined with a semi-implicit time discretization and a special treatment of boundary conditions in inviscid convective terms. In this way we obtain a numerical scheme requiring the solution of only one linear system on each time level.

The computational results show that the presented method is applicable to the numerical solution of inviscid compressible high-speed flow as well as flow with a very low

*This work is a part of the research project MSM 002162839 financed by the Ministry of Education of the Czech Republic.

†Charles University Prague, Faculty of Mathematics and Physics, Sokolovská 83, 18675 Praha 8, Czech Republic (feist@karlin.mff.cuni.cz).

‡Charles University Prague, Faculty of Mathematics and Physics, Sokolovská 83, 18675 Praha 8, Czech Republic (vaclav.kucera@email.cz)

Mach number at incompressible limit.

2. Continuous problem. For simplicity of the treatment we shall consider two-dimensional flow, but the method can be applied to 3D flow as well. The system of the Euler equations describing 2D inviscid flow can be written in the form

$$\frac{\partial \boldsymbol{w}}{\partial t} + \sum_{s=1}^{2} \frac{\partial \boldsymbol{f}_s(\boldsymbol{w})}{\partial x_s} = 0 \quad \text{in } Q_T = \Omega \times (0, T), \tag{2.1}$$

where $\Omega \subset I\!R^2$ is a bounded domain occupied by gas, $T > 0$ is the length of a time interval,

$$\boldsymbol{w} = (w_1, \ldots, w_4)^{\mathrm{T}} = (\rho,\, \rho v_1,\, \rho v_2,\, E)^{\mathrm{T}} \tag{2.2}$$

is the so-called state vector and

$$\boldsymbol{f}_s(\boldsymbol{w}) = (\rho v_s,\, \rho v_s v_1 + \delta_{s1} p,\, \rho v_s v_2 + \delta_{s2} p,\, (E + p)\, v_s)^{\mathrm{T}} \tag{2.3}$$

are the inviscid (Euler) fluxes of the quantity $\boldsymbol{w}$ in the directions x_s, $s = 1, 2$. We use the following notation: ρ – density, p – pressure, E – total energy, $\boldsymbol{v} = (v_1, v_2)$ – velocity, δ_{sk} – Kronecker symbol. The equation of state implies that

$$p = (\gamma - 1)\,(E - \rho|\boldsymbol{v}|^2/2). \tag{2.4}$$

Here $\gamma > 1$ is the Poisson adiabatic constant. The system (2.1)–(2.4) is *diagonally hyperbolic*. It is equipped with the initial condition

$$\boldsymbol{w}(\boldsymbol{x}, 0) = \boldsymbol{w}^0(x), \quad x \in \Omega, \tag{2.5}$$

and the boundary conditions, which are treated in Section 4. We define the matrix

$$\boldsymbol{P}(\boldsymbol{w}, \boldsymbol{n}) := \sum_{s=1}^{2} \boldsymbol{A}_s(\boldsymbol{w}) n_s, \tag{2.6}$$

where $\boldsymbol{n} = (n_1, n_2) \in \mathbb{R}^2,\ n_1^2 + n_2^2 = 1$ and

$$\boldsymbol{A}_s(\boldsymbol{w}) = \frac{D\boldsymbol{f}_s(\boldsymbol{w})}{D\boldsymbol{w}}, \qquad s = 1, 2, \tag{2.7}$$

are the Jacobi matrices of the mappings $\boldsymbol{f}_s$. It is possible to show that $\boldsymbol{f}_s,\ s = 1, 2$, are homogeneous mappings of order one, which implies that

$$\boldsymbol{f}_s(\boldsymbol{w}) = \boldsymbol{A}_s(\boldsymbol{w})\boldsymbol{w},\ s = 1, 2. \tag{2.8}$$

3. Discretization. Here we describe the construction of the discrete problem.

3.1. Space semidiscretization by the DGFEM. Let Ω_h be a polygonal approximation of Ω. By $\mathcal{T}_h$ we denote a partition of Ω_h consisting of various types of convex elements $K_i \in \mathcal{T}_h,\ i \in I$ ($I \subset Z^+ = \{0, 1, 2, \ldots\}$ is a suitable index set), e. g., triangles, quadrilaterals or in general convex polygons. (Let us note that in [6] and [8] it was shown that in the DGFEM also general nonconvex star-shaped polygonal elements can be used.) By Γ_{ij} we denote a common edge between two neighbouring elements K_i and K_j. Moreover, we set $s(i) = \{j \in I; K_j$ is a neighbour of $K_i\}$. The boundary $\partial\Omega_h$ is formed by a finite number of faces of elements K_i adjacent to $\partial\Omega_h$. We denote all these boundary faces by S_j, where $j \in I_b \subset Z^- = \{-1, -2, \ldots\}$. Now we set $\gamma(i) = \{j \in I_b; S_j$ is a face of $K_i \in \mathcal{T}_h\}$ and $\Gamma_{ij} = S_j$ for $K_i \in \mathcal{T}_h$ such that $S_j \subset \partial K_i,\ j \in I_b$. For K_i not containing any boundary face S_j we set $\gamma(i) = \emptyset$. Obviously, $s(i) \cap \gamma(i) = \emptyset$ for all $i \in I$. Now, if we write $S(i) = s(i) \cup \gamma(i)$, we have

$$\partial K_i = \bigcup_{j \in S(i)} \Gamma_{ij}, \qquad \partial K_i \cap \partial\Omega_h = \bigcup_{j \in \gamma(i)} \Gamma_{ij}. \tag{3.1}$$

The symbol $\boldsymbol{n}_{ij} = ((n_{ij})_1, (n_{ij})_2)$ will denote the unit outer normal to ∂K_i on the face Γ_{ij}. By h_{K_i} and $|K_i|$ we shall denote the diameter and the area, respectively, of an element $K_i \in \mathcal{T}_h$.

The approximate solution will be sought at each time instant t as an element of the finite-dimensional space

$$S_h = S^{r,-1}(\Omega_h, \mathcal{T}_h) = \{v; v|_K \in P^r(K)\ \forall K \in \mathcal{T}_h\}^4,$$

where $r \geq 0$ is an integer and $P^r(K)$ denotes the space of all polynomials on K of degree $\leq r$. Functions $v \in S_h$ are in general discontinuous on interfaces Γ_{ij}.

By $v|_{\Gamma_{ij}}$ and $v|_{\Gamma_{ji}}$ we denote the values of v on Γ_{ij} considered from the interior and the exterior of K_i, respectively.

In order to derive the discrete problem, we multiply (2.1) by a test function $\boldsymbol{\varphi} \in S_h$, integrate over any element $K_i,\ i \in I$, apply Green's theorem and sum over all $i \in I$. Then we approximate fluxes through the faces Γ_{ij} with the aid of a *numerical flux* $\boldsymbol{H} = \boldsymbol{H}(\boldsymbol{u}, \boldsymbol{w}, \boldsymbol{n})$ in the form

$$\int_{\Gamma_{ij}} \sum_{s=1}^{2} \boldsymbol{f}_s(\boldsymbol{w}(t))\, (n_{ij})_s \cdot \boldsymbol{\varphi}\, \mathrm{d}S \approx \int_{\Gamma_{ij}} \boldsymbol{H}(\boldsymbol{w}_h(t)|_{\Gamma_{ij}}, \boldsymbol{w}_h(t)|_{\Gamma_{ji}}, \boldsymbol{n}_{ij}) \cdot \boldsymbol{\varphi}\, \mathrm{d}S.$$

If we introduce the forms

$$(\boldsymbol{w}_h, \boldsymbol{\varphi}_h)_h = \int_{\Omega_h} \boldsymbol{w}_h \cdot \boldsymbol{\varphi}_h\, \mathrm{d}\boldsymbol{x}, \qquad \tilde{b}_h(\boldsymbol{w}_h, \boldsymbol{\varphi}_h) = \sigma_1 + \sigma_2, \tag{3.2}$$

where

$$\begin{aligned} \sigma_1 &= -\sum_{K \in \mathcal{T}_h} \int_K \sum_{s=1}^{2} \boldsymbol{f}_s(\boldsymbol{w}_h) \cdot \frac{\partial \boldsymbol{\varphi}_h}{\partial x_s}\, \mathrm{d}\boldsymbol{x}, \\ \sigma_2 &= \sum_{K_i \in \mathcal{T}_h} \sum_{j \in S(i)} \int_{\Gamma_{ij}} \boldsymbol{H}(\boldsymbol{w}_h|_{\Gamma_{ij}}, \boldsymbol{w}_h|_{\Gamma_{ji}}, \boldsymbol{n}_{ij}) \cdot \boldsymbol{\varphi}_h \mathrm{d}S, \end{aligned} \tag{3.3}$$

we can define an *approximate solution* of (2.1) as a function $\boldsymbol{w}_h$ satisfying the conditions

$$\begin{aligned} &\text{a)}\ \ \boldsymbol{w}_h \in C^1([0,T]; S_h), \\ &\text{b)}\ \ \frac{\mathrm{d}}{\mathrm{d}t}(\boldsymbol{w}_h(t), \boldsymbol{\varphi}_h)_h + \tilde{b}_h(\boldsymbol{w}_h(t), \boldsymbol{\varphi}_h) = 0, \qquad \forall\, \boldsymbol{\varphi}_h \in S_h,\ \ \forall\, t \in (0,T), \\ &\text{c)}\ \ \boldsymbol{w}_h(0) = \Pi_h \boldsymbol{w}^0, \end{aligned} \tag{3.4}$$

where $\Pi_h \boldsymbol{w}^0$ is the L^2-projection of $\boldsymbol{w}^0$ from the initial condition (2.5) on the space S_h. If we set $r = 0$, then we obviously obtain the finite volume method.

3.2. Time discretization. Relation (3.4), b) represents a system of ordinary differential equations which can be solved by a suitable numerical method. Usually, *Runge-Kutta schemes* are applied. However, they are conditionally stable and the time step is strongly limited by the CFL-stability condition. Therefore, we develop a semi-implicit time discretization, which is unconditionally stable and requires the solution of a linear system on each time level. This is carried out with the aid of a suitable partial linearization of the form $\tilde{b}_h$. In what follows, we consider a partition $0 = t_0 < t_1 < t_2 \dots$ of the time interval $(0, T)$ and set $\tau_k = t_{k+1} - t_k$. We use the notation $\boldsymbol{w}_h^k$ for the approximation of $\boldsymbol{w}_h(t_k)$.

On the basis of relation (2.8) and the use of the *Vijayasundaram numerical flux*, similarly as in [4], we construct the form

$$\begin{aligned} b_h(\boldsymbol{w}_h^k, \boldsymbol{w}_h^{k+1}, \boldsymbol{\varphi}_h) = &- \sum_{K \in \mathcal{T}_h} \int_K \sum_{s=1}^{2} \boldsymbol{A}_s(\boldsymbol{w}_h^k(\boldsymbol{x}))\boldsymbol{w}_h^{k+1}(\boldsymbol{x}) \cdot \frac{\partial \boldsymbol{\varphi}_h(\boldsymbol{x})}{\partial x_s}\,\mathrm{d}\boldsymbol{x} \\ &+ \sum_{K_i \in \mathcal{T}_h} \sum_{j \in S(i)} \int_{\Gamma_{ij}} \left[\boldsymbol{P}^+\left(\langle \boldsymbol{w}_h^k \rangle_{ij}, \boldsymbol{n}_{ij}\right) \boldsymbol{w}_h^{k+1}|_{\Gamma_{ij}} + \boldsymbol{P}^-\left(\langle \boldsymbol{w}_h^k \rangle_{ij}, \boldsymbol{n}_{ij}\right) \boldsymbol{w}_h^{k+1}|_{\Gamma_{ji}}\right] \cdot \boldsymbol{\varphi}_h \mathrm{d}S, \end{aligned} \tag{3.5}$$

which is linear with respect to the second and third variable. We use the notation $\langle \boldsymbol{w}_h^k \rangle_{ij} = (\boldsymbol{w}_h|_{\Gamma_{ij}} + \boldsymbol{w}_h|_{\Gamma_{ji}})/2$. Further, $\boldsymbol{P}^{\pm} = \boldsymbol{P}^{\pm}(\boldsymbol{w}, \boldsymbol{n})$ represents positive/negative part of the matrix $\boldsymbol{P}$ defined on the basis of its diagonalization (see, e. g. [10, Section 3.1]):

$$\boldsymbol{P} = \boldsymbol{T}\boldsymbol{D}\boldsymbol{T}^{-1},\ \boldsymbol{D} = \mathrm{diag}\ (\lambda_1, \dots, \lambda_4), \tag{3.6}$$

where $\lambda_1, \dots, \lambda_4$ are the eigenvalues of $\boldsymbol{P}$. Then we set

$$\begin{aligned} \boldsymbol{D}^{\pm} &= \mathrm{diag}\ (\lambda_1^{\pm}, \dots, \lambda_4^{\pm}), \\ \boldsymbol{P}^{\pm} &= \boldsymbol{T}\boldsymbol{D}^{\pm}\boldsymbol{T}^{-1}, \end{aligned} \tag{3.7}$$

where $\lambda^+ = \max\{\lambda, 0\}$ and $\lambda^- = \min\{\lambda, 0\}$.

On the basis of the above considerations we obtain the following semi-implicit scheme: For each $k \geq 0$ find $\boldsymbol{w}_h^{k+1}$ such that

$$\begin{aligned} &\text{a)}\ \ \boldsymbol{w}_h^{k+1} \in S_h, \\ &\text{b)}\ \ \left(\frac{\boldsymbol{w}_h^{k+1} - \boldsymbol{w}_h^k}{\tau_k}, \boldsymbol{\varphi}_h\right)_h + b_h(\boldsymbol{w}_h^k, \boldsymbol{w}_h^{k+1}, \boldsymbol{\varphi}_h) = 0,\ \forall\, \boldsymbol{\varphi}_h \in S_h,\ k = 0, 1, \dots, \\ &\text{c)}\ \ \boldsymbol{w}_h^0 = \Pi_h \boldsymbol{w}^0. \end{aligned} \tag{3.8}$$

This is a first order accurate scheme in time. It is also possible to construct a semi-implicit two step second order time discretization (see [4]). The linear algebraic system equivalent to (3.8), b) is solved by the GMRES method with a block diagonal preconditioning.

In order to obtain an accurate solution near curved boundaries, we use higher order isoparametric elements as in [1] or [3].

4. Boundary conditions. If $\Gamma_{ij} \subset \partial\Omega_h$, i. e. $j \in \gamma(i)$, it is necessary to specify the boundary state $\boldsymbol{w}|_{\Gamma_{ji}}$ appearing in the numerical flux $\boldsymbol{H}$ in the definition of the inviscid form b_h. The appropriate treatment of boundary conditions plays a crucial role in the solution of low Mach number flows.

On a fixed impermeable wall we employ a standard approach using the condition $\boldsymbol{v} \cdot \boldsymbol{n} = 0$ and extrapolating the pressure. On the inlet and outlet it is necessary to use nonreflecting boundary conditions transparent for acoustic effects coming from inside of Ω. Therefore, *characteristics-based* boundary conditions are used.

Using the rotational invariance, we transform the Euler equations to the coordinates $\tilde{x}_1$, parallel with the normal direction $\boldsymbol{n}$ to the boundary, and $\tilde{x}_2$, tangential to the boundary, neglect the influence of the states on elements that are not adjacent to Γ_{ij} and linearize the resulting system around the state $\boldsymbol{q}_{ij} = \boldsymbol{Q}(\boldsymbol{n}_{ij})\boldsymbol{w}|_{\Gamma_{ij}}$, where

$$\boldsymbol{Q}(\boldsymbol{n}_{ij}) = \begin{pmatrix} 1, & 0, & 0, & 0 \\ 0, & (n_{ij})_1, & (n_{ij})_2, & 0 \\ 0, & -(n_{ij})_2, & (n_{ij})_1, & 0 \\ 0, & 0, & 0, & 1 \end{pmatrix} \tag{4.1}$$

is the rotational matrix. Then we obtain the linear system

$$\frac{\partial \boldsymbol{q}}{\partial t} + \boldsymbol{A}_1(\boldsymbol{q}_{ij}) \frac{\partial \boldsymbol{q}}{\partial \tilde{x}_1} = 0, \tag{4.2}$$

for the vector-valued function $\boldsymbol{q} = \boldsymbol{Q}(\boldsymbol{n}_{ij})\boldsymbol{w}$, considered in the set $(-\infty, 0) \times (0, \infty)$ and equipped with the initial and boundary conditions

$$\begin{aligned} \boldsymbol{q}(\tilde{x}_1, 0) &= \boldsymbol{q}_{ij}, \qquad && \tilde{x}_1 \in (-\infty, 0), \\ \boldsymbol{q}(0, t) &= \boldsymbol{q}_{ji}, && t > 0. \end{aligned} \tag{4.3}$$

The goal is to choose $\boldsymbol{q}_{ji}$ in such a way that this initial-boundary value problem is well posed, i.e. has a unique solution. The method of characteristics leads to the following process:

Let us put $\boldsymbol{q}^*_{ji} = \boldsymbol{Q}(\boldsymbol{n}_{ij})\boldsymbol{w}^*_{ji}$, where $\boldsymbol{w}^*_{ji}$ is a prescribed boundary state at the inlet or outlet. We calculate the eigenvectors $\boldsymbol{r}_s$ corresponding to the eigenvalues λ_s, $s = 1, \dots, 4$, of the matrix $\boldsymbol{A}_1(\boldsymbol{q}_{ij})$, arrange them as columns in the matrix $\boldsymbol{T}$ and calculate $\boldsymbol{T}^{-1}$ (explicit formulae can be found in [10, Section 3.1]). Now we set

$$\boldsymbol{\alpha} = \boldsymbol{T}^{-1}\boldsymbol{q}_{ij}, \quad \boldsymbol{\beta} = \boldsymbol{T}^{-1}\boldsymbol{q}^*_{ji}. \tag{4.4}$$

and define the state $\boldsymbol{q}_{ji}$ by the relations

$$\boldsymbol{q}_{ji} := \sum_{s=1}^{4} \gamma_s \boldsymbol{r}_s, \quad \gamma_s = \begin{cases} \alpha_s, & \lambda_s \geq 0, \\ \beta_s, & \lambda_s < 0. \end{cases} \tag{4.5}$$

Finally, the sought boundary state $\boldsymbol{w}|_{\Gamma_{ji}}$ is defined as

$$\boldsymbol{w}|_{\Gamma_{ji}} = \boldsymbol{w}_{ji} = \boldsymbol{Q}^{-1}(\boldsymbol{n}_{ij})\boldsymbol{q}_{ji}. \tag{4.6}$$

5. Shock capturing. In the case of high speed flow, it is necessary to avoid the *Gibbs phenomenon* manifested by spurious overshoots and undershoots in computed quantities near discontinuities (shock waves, contact discontinuities). These phenomena do not occur in low Mach number regimes, but in transonic flow they cause instabilities in the numerical solution.

We avoid the Gibbs phenomenon by introducing a suitable stabilization terms, motivated by [7] and [12]. First we introduce the discontinuity indicator $g(i)$ proposed in [7] and defined by

$$g(i) = \int_{\partial K_i} [\rho_h^k]^2 \, \mathrm{d}S / (h_{K_i} |K_i|^{3/4}), \qquad K_i \in \mathcal{T}_h. \tag{5.1}$$

By $[u]|_{\Gamma_{ij}} = u_{ij} - u_{ji}$ we denote the jump on Γ_{ij} of a function $u \in S_h$. Further, we define the discrete indicator

$$G(i) = \begin{cases} 0, & g(i) < 1, \\ 1, & g(i) \geq 1. \end{cases}, \quad K_i \in \mathcal{T}_h. \tag{5.2}$$

Now, to the left-hand side of (3.8), b) we add the artificial viscosity form

$$\tilde{\beta}_h(\boldsymbol{w}, \boldsymbol{\varphi}) = \nu_1 \sum_{i \in I} h_{K_i} G(i) \int_{K_i} \nabla \boldsymbol{w} \cdot \nabla \boldsymbol{\varphi} \, \mathrm{d}\boldsymbol{x}, \tag{5.3}$$

where $\nu_1 \approx 1$. The stabilization form $\tilde{\beta}_h$ is treated semi-implicitly with $G(i) = G^k(i)$ computed from $\boldsymbol{w}_h^k$. Therefore, we write

$$\beta_h(\boldsymbol{w}_h^k, \boldsymbol{w}_h^{k+1}, \boldsymbol{\varphi}) = \nu_1 \sum_{i \in I} h_{K_i} G^k(i) \int_{K_i} \nabla \boldsymbol{w}_h^{k+1} \cdot \nabla \boldsymbol{\varphi} \, \mathrm{d}\boldsymbol{x}. \tag{5.4}$$

This form limits the order of accuracy only on elements lying in a small neighbourhood of a discontinuity. However, it appears that this is insufficient on strongly refined grids. Therefore, we propose to augment the left-hand side of (3.8), b) by adding the form

$$\tilde{J}_h(\boldsymbol{w}, \boldsymbol{\varphi}) = \nu_2 \sum_{i \in I} \sum_{j \in s(i)} \frac{1}{2}\big(G(i) + G(j)\big) \int_{\Gamma_{ij}} [\boldsymbol{w}] \cdot [\boldsymbol{\varphi}] \, \mathrm{d}S, \tag{5.5}$$

where $\nu_2 \approx 1$. In this way we penalize inter-element jumps in the vicinity of the shock wave. This form is again treated semi-implicitly, similarly as in (5.4). We set

$$J_h(\boldsymbol{w}_h^k, \boldsymbol{w}_h^{k+1}, \boldsymbol{\varphi}) = \nu_2 \sum_{i \in I} \sum_{j \in s(i)} \frac{1}{2}\big(G^k(i) + G^k(j)\big) \int_{\Gamma_{ij}} [\boldsymbol{w}_h^{k+1}] \cdot [\boldsymbol{\varphi}] \, \mathrm{d}S. \tag{5.6}$$

Thus, the resulting scheme reads:

$$\begin{aligned} &\text{a)} \quad \boldsymbol{w}_h^{k+1} \in S_h, \\ &\text{b)} \quad \left(\frac{\boldsymbol{w}_h^{k+1} - \boldsymbol{w}_h^k}{\tau_k}, \boldsymbol{\varphi}_h \right)_h + b_h(\boldsymbol{w}_h^k, \boldsymbol{w}_h^{k+1}, \boldsymbol{\varphi}_h) \\ &\qquad + \beta_h(\boldsymbol{w}_h^k, \boldsymbol{w}_h^{k+1}, \boldsymbol{\varphi}_h) + J_h(\boldsymbol{w}_h^k, \boldsymbol{w}_h^{k+1}, \boldsymbol{\varphi}_h) = 0, \ \forall \boldsymbol{\varphi}_h \in S_h, \ k = 0, 1, \ldots, \\ &\text{c)} \quad \boldsymbol{w}_h^0 = \Pi_h \boldsymbol{w}^0. \end{aligned} \tag{5.7}$$

This method successfully overcomes problems with the Gibbs phenomenon in the context of the semi-implicit scheme. It is important that $G(i)$ vanishes in regions where the solution is regular. Therefore, the scheme does not produce any nonphysical entropy in these regions (See Fig. 6.3).

6. Numerical examples. In order to show the robustness of the described technique with respect to the Mach number, we present computational results obtained for two types of compressible flow.

6.1. Low Mach number flow. First, the semi-implicit scheme (5.7) was applied to the solution of stationary inviscid low Mach number flow past a circular cylinder with the far field velocity parallel to the axis x_1 and the Mach number $M_\infty = 10^{-4}$. The computational domain has the form of a square with sides of the length equal to 20 diameters of the cylinder. We show here details of the flow in the vicinity of the cylinder. Fig. 6.1 shows isolines of the absolute value of the velocity for the compressible flow computed by scheme (5.7) with piecewise quadratic elements (i. e. $r = 2$), on a coarse mesh formed by 361 elements and on a fine mesh with 8790 elements, compared with the exact solution of incompressible flow (computed by the method of complex functions – see [9, Section 2.2.35]). The steady-state solution is obtained with the aid of the time stabilization for "$t \to \infty$".

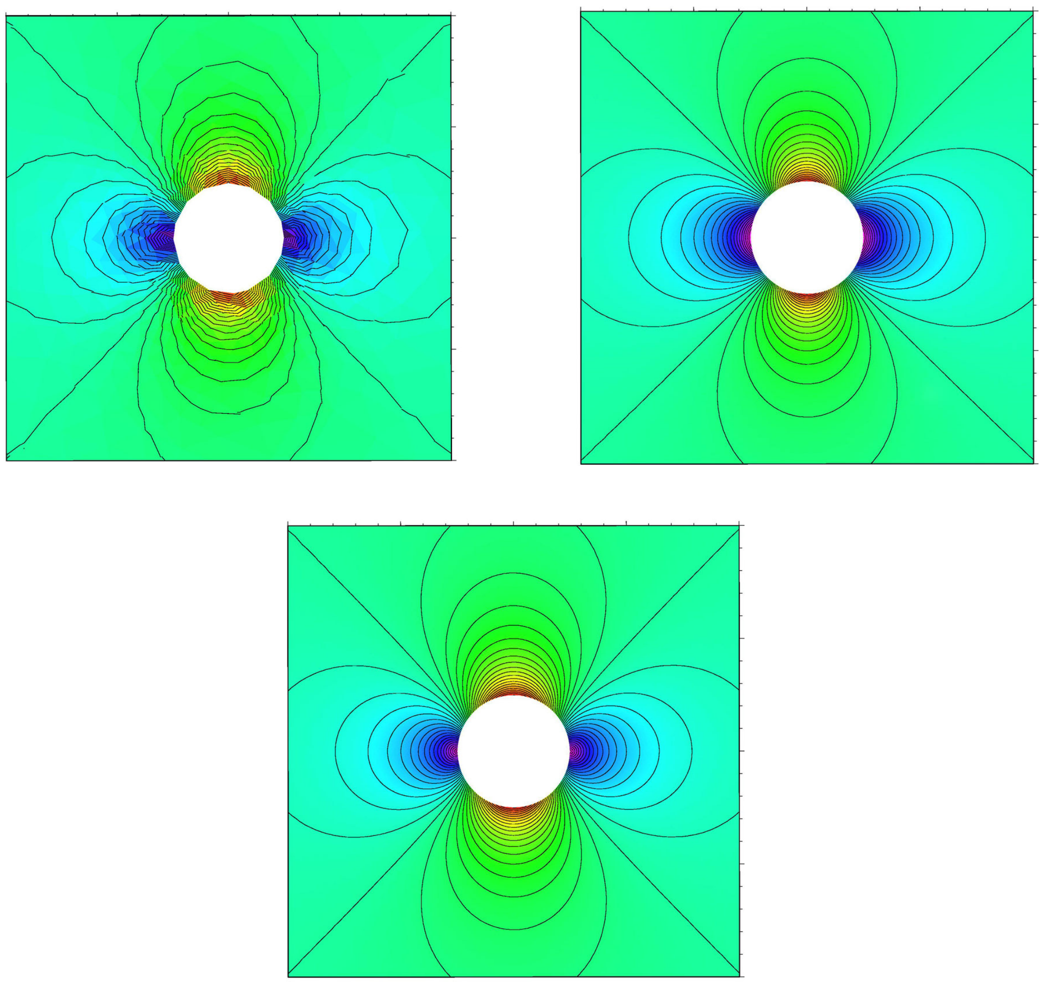

Fig. 6.1. *Velocity isolines for the approximate solution of compressible flow – coarse mesh (top left), fine mesh (top right), compared with the exact solution of incompressible flow (bottom).*

6.2. Transonic flow. The performance of shock capturing terms from Section 5 is tested on the GAMM channel with a 10% circular bump and the inlet Mach number equal to 0.67. The method (5.7) with piecewise quadratic elements is used and time stabilization for "$t \to \infty$" is applied for obtaining the steady-state solution. In this case a conspicuous shock wave is developed. In Fig. 6.2 the density distribution along the lower wall is shown. We see a well resolved discontinuity due to the shock wave. Moreover, we can see the so-called Zierep singularity (a small local maximum behind the shock) proving a good quality of the obtained numerical solution. The artificial viscosity forms β_h and J_h given by (5.4) and (5.6) eliminate the Gibbs phenomenon. Fig. 6.3 shows the entropy isolines. One can see that the entropy is produced only on the shock wave. This is caused by the use of the forms β_h and J_h, which are active only on elements lying in a small neighbourhood of discontinuities and do not influence the solution in areas, where the exact solution is regular.

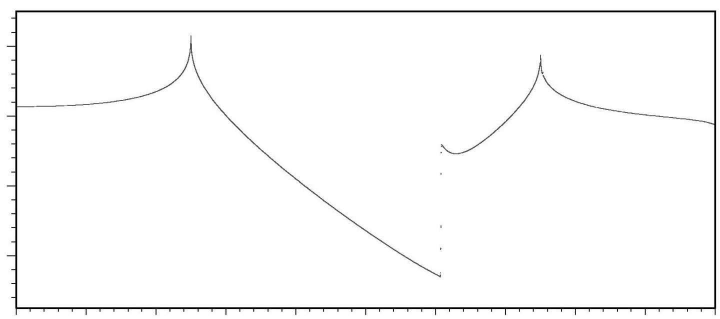

Fig. 6.2. *Transonic flow through the GAMM channel, density distribution on the lower wall.*

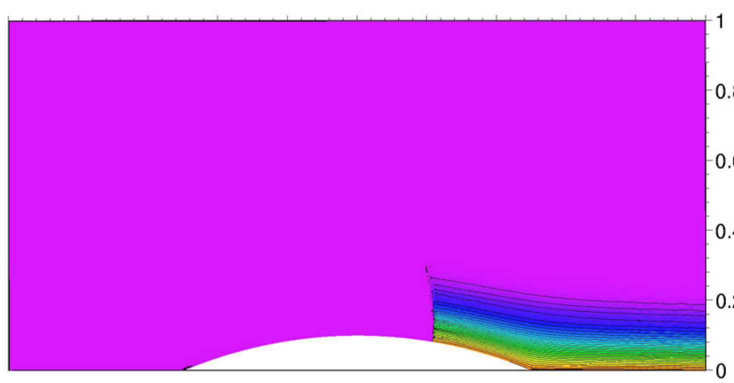

Fig. 6.3. *Transonic flow through the GAMM channel, entropy isolines.*

7. Conclusion. In this paper we have presented a new method for the numerical solution of the Euler equations describing inviscid compressible flow. The method allows the simulation of compressible flow with a wide range of Mach numbers – from very small values in the case of flows at incompressible limit, up to large Mach numbers for high speed transonic flows. Numerical experiments prove that the method is unconditionally stable. There are several important ingredients making the method robust with respect to the Mach number, without the necessity to modify the Euler equations:

– discontinuous Galerkin space discretization,

– semi-implicit time stepping,
– characteristic treatment of boundary conditions,
– suitable limiting of order of accuracy in the vicinity of discontinuities in order to avoid the Gibbs phenomenon,
– the use of isoparametric finite elements at curved parts of the boundary.

Our further goal is the extension of the presented technique to compressible viscous flow described by the full system of the compressible Navier-Stokes equations.

REFERENCES

[1] F. Bassi and S. Rebay, *High-order accurate discontinuous finite element solution of the 2D Euler equations*, J. Comput. Phys., **138** (1997), 251–285.

[2] E. Bauman, J. T. Oden, *A discontinuous hp finite element method for the Euler and Navier-Stokes equations*, Int. J. Numer. Methods Fluids, **31** (1999), 79–95.

[3] V. Dolejší and M. Feistauer, *On the discontinuous Galerkin method for the numerical solution of compressible high-speed flow*, in Numerical Mathematics and Advanced Applications, ENUMATH 2001, F. Brezzi, A. Buffa, S. Corsaro, and A. Murli, eds., Springer-Verlag Italia, Milano, 2003, 65–84.

[4] V. Dolejší and M. Feistauer, *A semi-implicit discontinuous Galerkin finite element method for the numerical solution of inviscid compressible flow*, J. Comput. Phys., **198** (2004), 727–746.

[5] V. Dolejší and M. Feistauer, *Error estimates of the discontinuous Galerkin method for nonlinear nonstationary convection-diffusion problems*, Numer. Func. Anal. Optimiz., **26**(3) (2005), 349–383.

[6] V. Dolejší, M. Feistauer and J. Hozman, *Analysis of semi-implicit DGFEM for nonlinear convection-diffusion problems on nonconforming meshes*, Comput. Methods Appl. Mech. Engrg. (in press), Preprint No. MATH-knm-2005/4, Charles University Prague, School of Mathematics (2005).

[7] V. Dolejší, M. Feistauer and C. Schwab, *On some aspects of the discontinuous Galerkin finite element method for conservation laws*, Math. Comput. Simul., **61** (2003), 333–346.

[8] V. Dolejší, M. Feistauer, and V. Sobotíková, *Analysis of the discontinuous Galerkin method for nonlinear convection–diffusion problems*, Comput. Methods Appl. Mech. Engrg., **194** (2005), 2709–2733.

[9] M. Feistauer, *Mathematical Methods in Fluid Dynamics*, Longman Scientific & Technical, Harlow, 1993.

[10] M. Feistauer, J. Felcman, and I. Straškraba, *Mathematical and Computational Methods for Compressible Flow.* Clarendon Press, Oxford, 2003.

[11] R. Hartmann and P. Houston, *Adaptive discontinuous Galerkin finite element methods for the compressible Euler equations*, J. Comput. Phys. **183** (2002), 508–532.

[12] J. Jaffre, C. Johnson and A. Szepessy, *Convergence of the discontinuous Galerkin finite element method for hyperbolic conservation laws*, Math. Models Methods Appl. Sci, **5**(3)(1995), 367–386.

[13] R. Klein, *Semi-implicit extension of a Godunov-type scheme based on low Mach number asymptotics 1: one-dimensional flow*, J. Comput. Phys., **121** (1995), 213–237.

[14] A. Meister and J. Struckmeier, *Hyperbolic Partial Differential Equations, Theory, Numerics and Applications*, Vieweg, Brauschweig – Wiesbaden, 2002.

[15] S. Roller, C.-D. Munz, K. J. Geratz and R. Klein, *The multiple pressure variables method for weakly compressible fluids*, Z. Angew. Math. Mech., **77** (1997), 481–484.

[16] J. J. W. van der Vegt and H. van der Ven, *Space-time discontinuous Galerkin finite element method with dynamic grid motion for inviscid compressible flows. I. General formulation*, J. Comput. Phys. **182** (2002), 546–585.

[17] G. Vijayasundaram, *Transonic flow simulation using upstream centered scheme of Godunov type in finite elements*, J. Comput. Phys., **63** (1986), 416–433.

[18] P. Wesseling, *Principles of Computational Fluid Dynamics*, Springer, Berlin, 2001.